Calculated Magnetic and Spin-Dependent Properties of FeCo/MgO/FeCo Tunnel Junction

P. Vlaic

University of Medicine and Pharmacy ''Iuliu Hatieganu'', Physics and Biophysics Department, RO 400023 Cluj-Napoca, Romania

Abstract

The magnetic tunnel junctions (MTJ) consisting of two ferromagnetic (FM) electrodes separated by a semiconducting or insulating spacer (S) (FM/S/FM) are attracting a great interest due to their applications in spin electronics. A particularly interesting system is represented by FeCo/MgO/FeCo MTJ that present a large tunneling magnetoresistance effect (TMR) [1-5] and also exhibit a broad range of magnetic properties with the variation of the film thickness.

In the present work the electronic structure, magnetic behavior and transport properties of M/MgO/M MTJ with M=Fe, Co and FeCo are studied.

For all systems the electronic properties and magnetic behavior of interface M atoms are strongly influenced by the M/MgO interface geometry. In case of FeCo/MgO/FeCo heterostructures the highest values of the iron and cobalt magnetic moments are obtained for experimental interface configuration with Fe(Co) atoms sitting above O ones (m_{Fe}=2.9 μ_B and m_{Co}=1.9 μ_B).

A small antiferromagnetic (AFM) coupling is observed between Fe electrodes, in agreement with experimental data [6-7]. For $Fe_{1-x}Co_x$/MgO/$Fe_{1-x}Co_x$ series, a transition from FM to antiferromagnetic (AFM) state is obtained for x=0.7.

High values of TMR ratio are obtained for $Fe_{1-x}Co_x$/MgO/$Fe_{1-x}Co_x$ systems. TMR=275% for pure Fe electrodes and decrease down to 70% for Co one.

Bulk Properties of MgO

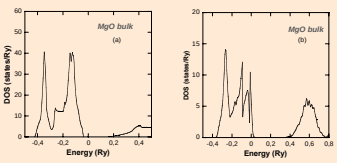

Fig. 3 DOS for bulk MgO

The electronic structure calculations were performed for following electronic configurations: Mg: core 3s², O: core + 2p⁴ (Exp. Gap MgO 7.8 eV(0.57 Ry)).

The total energy calculations gave an equilibrium lattice constant of 4.05 Å that is only 3.6 % smaller than the experimental value of 4.2 Å.

The main inconvenient of the LDA approximation is the reduction of the calculated band gap compared with the experimental value.

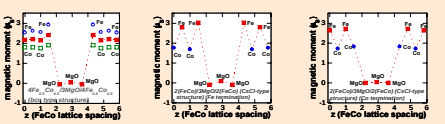

Fig. 8 Layer resolved magnetic moments for $4Fe_{0.5}Co_{0.5}$/3MgO/$4Fe_{0.5}Co_{0.5}$ and 2(FeCo)/3MgO/2(FeCo) systems

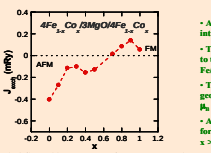

Fig. 9 Composition dependence of the exchange coupling in $Fe_{1-x}Co_x$/3MgO/$Fe_{1-x}Co_x$ series

- A small charge transfer was evidenced at the M/MgO interface.
- The magnetic behavior of the interface Fe atoms is sensitive to the interface configuration. Thus, M_{Fe}=2.87 μ_B at the Fe/OMg interface and M_{Fe}=2.78 μ_B at the Fe/MgO interface.
- The Co magnetic behavior is less sensitive to the interface geometry: M_{Co}=1.91 μ_B at the Co/OMg interface and M_{Co}=1.87 μ_B at the Co/MgO interface.
- A transition from the AFM state to the FM one is obtained for the exchange coupling for $Fe_{1-x}Co_x$/3MgO/$Fe_{1-x}Co_x$ series x >0.7.

4. Transport Properties

For a trilayer system sandwiched between two semi-infinite leads, the conductance G^X *for spin* σ *and magnetic state X (X=FM or AFM) may be expressed via the transmission function as:*

$$G^X_\sigma = \frac{e^2}{h}\frac{1}{N_{\vec{k}}}\sum_{\vec{k}}\left[dE\left(-\frac{df}{dE}\right)T^X(\vec{k}_{\vec{k}},E)\right] \quad (1)$$

where $N_{\vec{k}}$ *is the number of* $k_{\vec{k}}$ *points in the surface Brillouin zone, e the electron charge, h the Planck constant,* $f(E)$ *the Fermi-Dirac distribution function and T represent the transmission coefficient of the magnetic state X and spin* σ *and may be computed using the surface Green's function of the leads and that of the active region of system [10].*

The TMR ratio for a trilayer system where the consecutive magnetic layers may be coupled either FM or AFM may be expressed as:

$$TMR = \frac{R_{AFM}}{R_{FM}} - 1 = \frac{G_{FM}}{G_{AFM}} - 1 \quad (2)$$

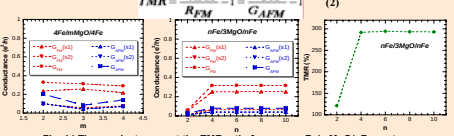

Fig. 14 The conductance ant the TMR ratio for some nFe/mMgO/nFe systems

$$\frac{dI_{\uparrow\uparrow}}{dV} = G_{\uparrow\uparrow}\cos^2(\theta/2) + G_{\uparrow\downarrow}\sin^2(\theta/2) \qquad \frac{dI_{\uparrow\downarrow}}{dV} = G_{\downarrow\downarrow}\cos^2(\theta/2) + G_{\downarrow\uparrow}\sin^2(\theta/2)$$

$$\frac{dI_{\downarrow\downarrow}}{dV} = G_{\uparrow\uparrow}\cos^2(\theta/2) + G_{\downarrow\uparrow}\sin^2(\theta/2) \qquad \frac{dI_{\downarrow\uparrow}}{dV} = G_{\downarrow\downarrow}\cos^2(\theta/2) + G_{\uparrow\downarrow}\sin^2(\theta/2) \quad (6)$$

The in-plane torkance $\left(\frac{d\tau}{dV}\right)$ **is given by:**

$$\frac{d\tau_{\vec{u}}}{dV} = \frac{\hbar}{4e}(G_{\uparrow\uparrow} - G_{\downarrow\downarrow} + G_{\uparrow\downarrow} - G_{\downarrow\uparrow})\sin(\theta) \quad (7)$$

$$\left(\frac{dI}{dV}\right)_P = G_{\uparrow\uparrow} + G_{\downarrow\downarrow} \qquad \left(\frac{dI}{dV}\right)_{AP} = G_{\uparrow\downarrow} + G_{\downarrow\uparrow} \quad (8)$$

$$\frac{d\tau_{\vec{u}}}{dV}(V=0) = \frac{\hbar}{4e}\frac{2P}{1+P^2}\sin(\theta)\left(\frac{dI}{dV}\right)_P \quad (9)$$

where P_x is the tunneling polarization

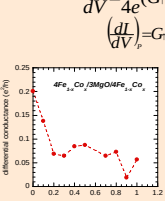

Fig. 19 Differential conductance versus composition for $Fe_{1-x}Co_x$/3MgO/$Fe_{1-x}Co_x$ series

Computational Details

Electronic Structure Calculations:

- Performed by means of a first principle Green's function technique for surfaces and interfaces, based on the tight-binding linear muffin-tin orbital method in its atomic sphere approximation *(TB-LMTO-ASA)* [8]. The local spin density approximation *(LSDA)* was used for exchange correlation potential within Vosko-Wilk-Nusair parametrisation [9].

Interdiffusion at the interfaces and chemical disorder:

- Use of the coherent potential approximation *(CPA)* [8].

The Conductance and the TMR Ratio:

- The calculations are performed in the ballistic limit in the current perpendicular-to-plane geometry *(CPP)* by means of the transmission matrix formulation of the *Kubo-Landauer's formalism* [10].

The self consistent calculations were performed for 648 k-points in the irreducible part of the 2D Brillouin zone. The convergence of the total energy, charge transfer, magnetic moment and tunneling magnetoresistance ratio (TMR) with respect to the k point sampling has been checked and the total energy is converged within 0.1 mRy.

Results

1. Electronic Structure and Magnetic properties Versus the Lattice Spacing

- Total energy calculations versus lattice spacing were performed for all studied systems for two configurations of M/MgO interfaces: (a) M sitting above O (M/OMg interface) and respectively for M located atop Mg atoms (M/MgO interface). All calculations shown that Fe/OMg interface is the most stable.

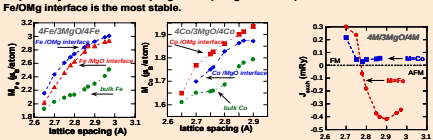

Fig. 4 Interface and bulk Fe and Co magnetic moments versus lattice spacing for 4Fe/3MgO/4Fe and 4Co/3MgO/4Co systems

Fig. 5 Interlayer exchange coupling versus lattice spacing

- Magnetic moments are sensitive at interface configuration.
- Highest values of magnetic moments are obtained for M/OMg interfaces

$J_{exch}=E_{total}(AFM)-E_{total}(FM)$

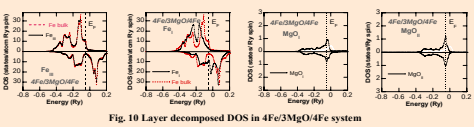

Fig. 10 Layer decomposed DOS in 4Fe/3MgO/4Fe system

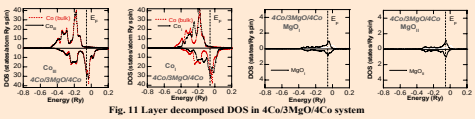

Fig. 11 Layer decomposed DOS in 4Co/3MgO/4Co system

- The DOS of Fe and Co atoms away from M/MgO interfaces are bulk-like.
- At the M/GaAs interfaces the majority-spin DOS are shifted toward lower energies while the minority-spin DOS are shifted toward higher energies and a maximum is observed near the Fermi level.

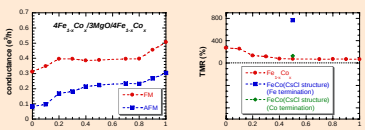

Fig. 15 Composition dependence of the conductance and TMR ratio in $Fe_{1-x}Co_x$/3MgO/$Fe_{1-x}Co_x$ series

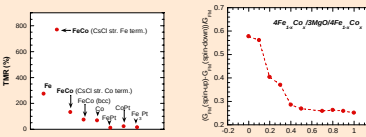

Fig. 16 TMR ratio for some M/MgO/M MTJ

Fig. 17 Current spin polarization versus composition for $Fe_{1-x}Co_x$/3MgO/$Fe_{1-x}Co_x$ series

Conclusions

- The results show the formation of sharp M/MgO interfaces with weak interactions between M (M=Fe, Co, $Fe_{1-x}Co_x$) and MgO layers.
- The interface Fe and Co magnetic moments are enhanced over the corresponding bulk values i. e., m_{Fe}=2.9 μ_B, m_{Co}=1.9 μ_B at Fe(Co)/MgO interfaces
- At the Fe/MgO interface the magnetic behavior of iron atoms is sensitive to the interface configuration while in the case of Co systems, it is less influenced by the interface geometry.
- The exchange coupling for the $Fe_{1-x}Co_x$/MgO/$Fe_{1-x}Co_x$ series is composition dependent and a transition from the AFM state to the FM one is obtained for x≥0.7.
- The TMR ratio of $Fe_{1-x}Co_x$/MgO/$Fe_{1-x}Co_x$ series decrease with increasing Co content from 275% for x=0 down to 70% for x=1.
- For the FeCo/MgO/FeCo system (FeCo in CsCl-type structure) the transport properties are sensitive to the terminations of the FeCo magnetic slab.
- The highest value of the TMR ratio was obtained for the FeCo/MgO/FeCo system (FeCo in CsCl-type structure) in the case of Fe termination.

M/MgO/M Multilayer Structures with M=Fe, Co and $Fe_{1-x}Co_x$

Studied Systems:

/(semi-infinite) M (001)/*n*M/*m*MgO/*n*M/M (001) (semi-infinite)/ (M=Fe, Co and FeCo)

n, m=numbers of atomic monolayers *(ML)* of either M or MgO (in present work n=4, m=3).
The bcc-type structure is assumed for $Fe_{1-x}Co_x$ magnetic slabs and the NaCl-type structure for the MgO spacer (Fig.1). For Fe0.5Co0.5, the CsCl-type structure is also considered.
A perfect lattice matching is assumed between M and MgO (a_{MgO}= a_{Fe}) (a_{Fe}=2.867 Å).
The MgO layers are rotated with 45° with respect to the Fe ones.
Each M monolayer consist of only one position while the MgO ML consist of two non-equivalent positions occupied by Mg and O atoms.
Due to the open structure of the MgO spacer, two empty spheres were introduced between MgO planes as well as between M and MgO layers at the M/MgO interfaces.

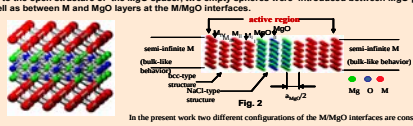

Fig. 1 The atomic structure of M/MgO interfaces (M=Fe, Co, and FeCo)

Fig. 2

In the present work two different configurations of the M/MgO interfaces are considered:
1. M atoms sitting above the O ones (exp. observed) (M/OMg int).
2. M atoms sitting above the Mg ones (M/MgO interface)

Fig. 6 Interface and bulk Fe and Co magnetic moments versus lattice spacing for $4Fe_{0.5}Co_{0.5}$/3MgO/$4Fe_{0.5}Co_{0.5}$ systems

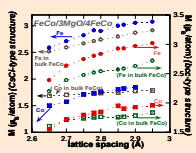

- A transition from FM to the AFM coupling with increasing lattice parameter is obtained for Fe system while the Co one remains always more stable in the FM state.

2. Ground-State Electronic and Magnetic properties.

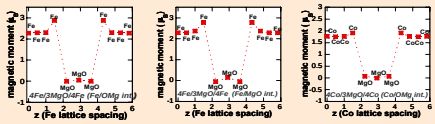

Fig. 7 Layer resolved magnetic moments for 4Fe/3MgO/4Feand 4Co/3MgO/4Co systems

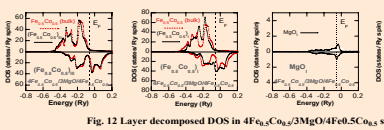

Fig. 12 Layer decomposed DOS in $4Fe_{0.5}Co_{0.5}$/3MgO/4Fe0.5$Co_{0.5}$ system

3. Effect of the Interdiffusion at the M/MgO Interfaces

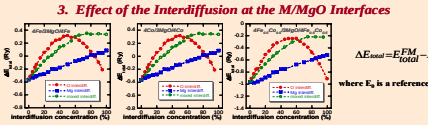

$\Delta E_{total}=E^{FM}_{total}-E_0$

where E_0 is a reference value

Fig. 13 Total energy dependence on the interdiffusion concentration for 4M/3MgO/4M systems (M=Fe, Co and $Fe_{0.5}Co_{0.5}$)

- Interdiffused interface extends over two neighboring layers in both O ($M_{1-x}O_x$)/(M_xO_{1-x}) and Mg ($M_{1-x}Mg_x$)/(M_xMg_{1-x}) interdiffusion as well as in the mixed case ($M_{1-(x'+x'')}O_{x'}Mg_{x''}$)/($M_{x'}O_{1-x'}$)($M_{x''}Mg_{1-x''}$)

5. Spin-Transfer Torque

Magnetization dynamics is described by the modified Landau-Lifshitz-Gilbert equation.

$$\frac{d\vec{M}}{dt} = \gamma(\vec{M}\times\vec{H}_{eff}) + \frac{\alpha}{M_s}\vec{M}\times\frac{d\vec{M}}{dt} + \frac{\gamma a_J(\theta)}{M_s}\vec{M}\times(\vec{M}\times\vec{P}) \quad (3)$$

Where **γ** represents the giromagnetic ratio, **α** is the Gilbert dumping parameter, $\vec{H}_{eff}$ is an effective field acting on the system, M/M_s is the reduced magnetization and $\cos(0)=\vec{M}\cdot\vec{P}$.

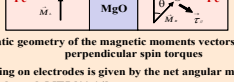

Fig. 18 Schematic geometry of the magnetic moments vectors and the in-plane and perpendicular spin torques

The spin torque acting on electrodes is given by the net angular momentum transferred by the current passing through MTJ [11-14]:

$$\vec{\tau}_L + \vec{\tau}_R = \frac{\hbar}{2e}\left[(I_{R\uparrow} - I_{R\downarrow})\hat{r} - (I_{L\uparrow} - I_{L\downarrow})\hat{r}\right] \quad (4)$$

where the majority and minority spin currents may be expressed in terms of conductances $G_{\sigma\sigma'}$ (σ, σ'= ↑, ↓) (Eq. (6)):

$$\tau_{R//} \equiv \tau = \frac{\hbar}{2e}\frac{\left[(I_{L\uparrow} - I_{L\downarrow}) - (I_{R\uparrow} - I_{R\downarrow})\cos(\theta)\right]}{\sin(\theta)} \quad (5)$$

References

[1] S. S. P. Parkin, C. Kaiser, A. Panchula, P. M. Rice, B. Hughes, M. Samant and S. H. Yang, Nat. Mater. 3, 862 (2004).
[2] S. Yuasa, T. Nagahama, A. Fukushima, Y. Suzuki and K. Ando, Nat. Mater. 3, 868 (2004).
[3] M. Bowen, V. Cros, F. Petroff, A. Fert, C. M. Boubeta, J. L. Costa-Krämer, J. V. Anguita, A. Cebollada, F. Briones, J. M. de Teresa, L. Morellón, M. R. Ibarra, F. Güell, F. Peiró and A Cornet, Appl. Phys. Lett.79, 1655 (2001).
[4] W. H. Butler, X. -G. Zhang, T.C. Schulthess and J. M. MacLaren, Phys. Rev. B 63, 054416 (2001).
[5] K. D. Belashchenko, J. Velev and E. Y. Tsymbal, Phys. Rev. B 72, 140404 (2005).
[6] J. Faure-Vincent, C. Tiusan, C. Bellouard, E. Popova, M. Hehn, F. Montaigne and A. Schul, Phys. Rev. Lett. 89, 107206 (2002).
[7] T. Katayama, S. Yuasa, J. Velev, M. Y. Zhuravlev, S. S. Jaswall, E. Tsymbal, Appl. Phys. Lett. 89, 112530 (2006).
[8] I. Turek, V. Drchal, J. Kudrnovský, M. Šob, and P. Weinberger in *Electronic Structure of Disordered Alloys, Surfaces and Interfaces* (Kluwer Academic Publishers, 1997).
[9] S. H. Vosko, L. Wilk, and M. Nusair, Can. J. Phys. 58 (1980) 1200.
[10] J. Kudrnovský, V. Drchal, C. Blaas, P. Weinberger, I. Turek, and P. Bruno, Phys. Rev. B 62 (2000) 15084.
[11] J. C. Slonczewski, Phys. Rev. B 39 (1989) 6995.
[12] J. C. Slonczewski, Phys. Rev. B 71 (2005) 024411.
[13] J. C. Slonczewski and J. Z. Sun, J. Magn. Magn. Mater. 310 (2007) 169.
[14] J. Z. Sun, D. C. Ralph, J. Magn. Magn. Mater 320 (2008) 1227.